



# Performance Analysis of IIR and FIR Filters for 5G Wireless Networks

Akram Muhammad Razee<sup>1\*</sup>, Rudzidatul Akmam Dziauddin<sup>2</sup>, Marwan Hadri Azmi<sup>3</sup>, Sajaa Kh Sadon<sup>4</sup>

<sup>1</sup>Razak Faculty of Technology and Informatics,  
Universiti Teknologi Malaysia, Jalan Sultan Yahya Petra,  
Kuala Lumpur, 54100, Malaysia.

<sup>2</sup>Ubiquitous Broadband Access Networks (U-BAN)  
Razak Faculty of Technology and Informatics,  
Universiti Teknologi Malaysia, Jalan Sultan Yahya Petra,  
Kuala Lumpur, 54100, Malaysia.

<sup>3</sup>Wireless Communication Centre (WCC),  
School of Electrical Engineering, Faculty of Engineering,  
Universiti Teknologi Malaysia, 81310 Skudai, Johor, Malaysia.

<sup>4</sup>Telekom Malaysia Research & Development (TM R&D)  
TM Innovation Centre  
63000 Cyberjaya, Selangor, Malaysia.

\*Corresponding Author

DOI: <https://doi.org/10.30880/ijie.2018.10.07.025>

Received 25 October 2018; Accepted 25 November 2018; Available online 30 November 2018

**Abstract:** This paper analyses the performances of the Infinite Impulse Response (IIR) and Finite Impulse Response (FIR) filters. By studying the relationship between filter responses with filter orders and delay, the goal is to choose feasible filters that can accommodate more carriers in a bandwidth thus, the spectral efficiency can be increased. For IIR filtering, we employ filters namely Butterworth, Chebyshev, and Elliptic, while the Equiripple, Bohman, and Hamming are studied for FIR filtering. We evaluate these filters in terms of magnitude response, phase response and group delay, and identify the minimum filter order that characterized nearly to an ideal filter response. The results show that the IIR filter has a steep transition region when compared to the FIR filters under the similar order. Our performance analysis showed that the IIR filters, with similar filter order of FIR filters, have also the fastest roll-off, small transition region, and low implementation cost. On the other hand, the FIR filters have linear phase response that related to group delay. Finally, our analysis concluded that Elliptic able to suppress the sidelobes with a minimum order of  $10^{\text{th}}$  and Equiripple have the fastest roll-off and narrowest transition region compare to other tested FIR filter. Thus, make these two types of filter feasible candidates to be implemented in 5G wireless networks.

**Keywords**—IIR, FIR, Butterworth, Chebyshev, Elliptic, Equiripple, Bohman, Hamming, Magnitude Response.

## 1. Introduction

A filter can be considered as a network or system that adopted signal processing and communication circuit systems to recover the signals within the transmitted bandwidth and to remove the unwanted parts of the signal such as Out-Of-Band (OOB) frequency components, overshoot, and random noise. As a result, filters are frequency selective circuit

\*Corresponding author: [akram3@live.utm.my](mailto:akram3@live.utm.my)

2018 UTHM Publisher. All right reserved.

[penerbit.uthm.edu.my/ojs/index.php/ijie](http://penerbit.uthm.edu.my/ojs/index.php/ijie)

allowing only the desired frequency to pass, while others are attenuated at parameters that have been assigned [1]. In 5G networks [2], [3], designing near optimal filter response is crucial for reaching 5G high-data rate enhanced mobile broadband and ultra-reliable low-latency communications requirements [4]. One way to achieve this demanding 5G requirement is to improve the spectral efficiency by deploying better filters that can reduce the OOB emission [5], [6]. OOB emissions reduce the overall system performance as they either cause interference to the neighboring frequency bands or require maintenance of substantial guardbands to limit this interference. Choosing the suitable filter for the system depends on the degree of the filter order and phase delay [7]. Using higher filter orders increases the processing delay. This is because high filter orders increase the number of poles, which then increases the implementation cost. The drawback of having a high phase delay is that the information can be miss interpreted at the output. As of the result from selecting the right filter is that the spectrum efficiency improved while eliminating noise, bit error rate, side lobes, and Intersymbol Interference (ISI) [8].

On an Internet of Thing (IoT) era [9], [10], the filtering techniques are vital to some applications that need low error rate data and low latency, such as in military, autopilot car, aircraft, and medical field. Digital filters can be categories as Infinite Impulse Response (IIR) Digital filters and Finite Impulse Response (FIR) Digital Filters [11], [12]. The IIR filters are digital filters with infinite impulse response and have a feedback, which is a recursive part of a filter [13]. Due to this property, IIR filters tend to have better frequency response rather than FIR filter with the same order [14]. However, due to the feedback, each output of IIR filtering need to be individually calculated and used to interpolate the next sample during the filtering process. Nevertheless, most IIR filters are likely to suffer phase delay and group delay. On the other hand, the FIR filters can be decimated or interpolated the samples rate depends on the applications, thus providing an important computational efficiency and suited to a multi-rate application like high-quality data to low-quality data that have different sample rate. The disadvantage of FIR is that the filter response characteristic. Several recent optimization methods to design the FIR and IIR and filter banks are reviewed. Here [15] the work considers the stability of the weighted least squares filter by studying its filter coefficients. They concluded that the optimum filter design framework plays important roles because of the huge effects on the impulse response. The work of [16]-[18] then explored the design of similar types of the filter by looking and analysing only on its magnitude response with few orders. Similar studies are performed in [19] by analysing only IIR filters and in [20] for FIR filters.

As most previous work designing only in a specific type of filter, this work focusses to provide an overall filtering performance that can be applied in filtered-OFDM (f-OFDM). Specifically, we simulate the filter response with different filter orders and investigate both FIR and IIR performances that are feasible for the f-OFDM system. Our work covers the performances of IIR filters, namely Butterworth, Chebyshev and Elliptic, and the FIR filters named Equiripple, Bohman, and Hamming. These filters are chosen due to their unique filtering techniques and differences property that can suppress side lobes and minimize transition region [21]. This allows the accommodation of more multi-carrier waveforms within the system bandwidth and hence increases the transmission rates while decreasing bit error rate caused by phase delay. Finally, we evaluate the filters subject to their magnitude response, phase response, group delay and the minimum filter order and the comparison is made with an ideal filter response

The paper is organized as follows. Sections 2 and 3 define and formulate the studied IIR and FIR filters, respectively. Section 4 presents the filter parameter considered in this work. Results and discussion are presented in Section 5. Finally, Section 6 concludes the paper.

## 2. Infinite Impulse Response (IIR)

In this section, we cover equation and property for all three IIR filters, namely Butterworth, Chebyshev and, Elliptic.

### 2.1 Butterworth

The Butterworth filter has the fewest property compare with the other filters tested in this paper. Butterworth filter can be derived from:

$$G(\omega) = \frac{1}{\sqrt{1+(\omega/\omega_c)^{2n}}} \quad (1)$$

where  $\omega$  is the angular of frequency in radian,  $\omega_c$  is the cutoff frequency and  $n$  is the number of pole or element in filter [22].

### 2.2 Chebyshev

The gain response of Chebyshev  $G(\omega)$  can be derived by  $\omega$  angular response of nth order low-pass filter is equal to the value of transfer function  $H_n(s)$  evaluated at  $s = j\omega$

$$G_n(\omega) = |H_n(j\omega)| = \frac{1}{\sqrt{1+\varepsilon^2 T_n^2(\frac{\omega}{\omega_0})}} \quad (2)$$

where  $\epsilon$  is the ripple factor,  $\omega$  is the angular frequency  $\omega_0$  is the cutoff frequency and  $T_n$  is Chebyshev polynomial of  $n$ th order [23].

### 2.3 Elliptic

The gain response of Elliptic of angular frequency  $\omega$  is given by:

$$G_n(\omega) = \frac{1}{\sqrt{1 + \epsilon^2 R_n^2(\xi, \omega/\omega_0)}} \tag{3}$$

where,  $R_n$  is the  $n$ -th order elliptic function,  $\omega$  is the angular frequency,  $\omega_0$  is the cutoff frequency,  $\epsilon$  is the ripple factor, and  $\xi$  is the selective factor [24].

### 3. Finite Impulse Response

In this section, we cover equation and property for all three FIR filters, namely Equiripple, Bohman and Hamming.

#### 3.1 Equiripple

The Equiripple filter is defined using the Remez algorithm with function  $f$  to be approximated and a set  $X$  of  $n + 2$  sample points  $x_1, x_2, \dots, x_{n+2}$  in the approximation interval. The linear system of equation to be satisfied is:

$$b_0 + b_{1x_i} + \dots + b_n x_i^n + (-1)^2 E = f(x_i) \tag{4}$$

(where  $i = 1, 2, \dots, n + 2$ ),

for the unknowns;  $b_0, b_1 \dots b_n$  and  $E$ , use the  $b_i$  as coefficients of polynomial  $P_n$  and then find the set of  $M$  of points error  $|P_n(x) - f(x)|$  if the errors at every  $m \in M$  are equal magnitude and alternate in sign, then  $P_n$  is the minimax approximation polynomial, if not replace  $X$  with  $M$  and from the start again with linear system equation [25].

#### 3.2 Window

Sufficiently large signals are difficult to analyze statistically because statistical calculations require all points to be available for analysis. In order to avoid these problems, the total data will be chunked into a smaller size, through a process called windowing that involves simply truncating the data set before and after the window. In this paper, we employ Bohman and Hamming windows for comparison.

##### 3.2.1 Bohman

A convolution of two semi-periods of a cosine function, the coefficients of a Bohman window are computed from the following equation where,  $n$  = current window length and  $N$  = total window length [26].

$$w(n) = \left( 1 - \frac{|n - \frac{N-1}{2}|}{\frac{N-1}{2}} \right) \cos\left( \pi \frac{|n - \frac{N-1}{2}|}{\frac{N-1}{2}} \right) + \frac{1}{\pi} \sin\left( \pi \frac{|n - \frac{N-1}{2}|}{\frac{N-1}{2}} \right); \tag{5}$$

$$0 \leq n \leq N - 1$$

##### 3.2.2 Hamming

A filter that is designed with the Hamming window has minimum stopband attenuation, which is sufficient for most implementations of digital filters. The coefficients of a Hamming window are computed from the following equation where,  $n$  = total window length [27].

$$w(n) = 0.54 - 0.46 \cos \frac{2\pi n}{N-1}; \tag{6}$$

$$0 \leq n \leq N - 1$$

### 4. Design Parameter

All Table 1 shows the general filter parameters and frequencies used across all filter orders considered in our simulations. The frequencies sampling is set at 4.8 MHz for standard audio sampling rate and by increasing the sampling

up to 4.8Thz it will not affect the filter output design and filter coefficient, while all the filter response types are bandpass. The remaining filter specifications are listed in Table 2 for every filter.

**Table 1 – Filter Parameter and Coefficients.**

Parameter	Frequency/Magnitude
Frequency sampling, $F_s$	48000 kHz
First cutoff frequency, $F_{c1}$	8400 kHz
Second cutoff frequency, $F_{c2}$	13200 kHz
Beginning of the passband, $F_{pass1}$	9600 kHz
End of the passband, $F_{pass2}$	12000 kHz
Passband ripple, $A_{pass}$	1 dB
End of the first stopband, $F_{stop1}$	7200 kHz
Beginning of the second, $F_{stop2}$	14400 kHz
Weight in the first stopband, $W_{stop1}$	1 dB
Weight in the second stopband, $W_{stop2}$	1 dB
Weight in the passband, $W_{pass}$	1dB
Frequency sampling, $F_s$	48000 kHz
First cutoff frequency, $F_{c1}$	8400 kHz
Second cutoff frequency, $F_{c2}$	13200 kHz
Beginning of the passband, $F_{pass1}$	9600 kHz
End of the passband, $F_{pass2}$	12000 kHz
Passband ripple, $A_{pass}$	1 dB
End of the first stopband, $F_{stop1}$	7200 kHz

The frequency and magnitude specifications for each filter used are summarized in Table 2.

**Table 2 – Frequency and Magnitude Specifications.**

Filter Type	Design	Property	Magnitude Specification
Butterworth	IIR	$F_s, F_{c1}$ and $F_{c2}$	Attenuation Fix at 3 db
Elliptic	IIR	$F_s, F_{pass1}$ and $F_{pass2}$	$A_{stop}$ and $A_{pass}$
Chebyshev	IIR	$F_s, F_{pass1}$ and $F_{pass2}$	$A_{pass}$
Equiripple	FIR	$F_s, F_{stop1}, F_{pass1}, F_{pass2}$ and $F_{stop2}$	$W_{stop1}, W_{stop2}$ and $W_{pass}$
Bohman	FIR	$F_s, F_{c1}$ and $F_{c2}$	Attenuation Fix at 6 db
Hamming	FIR	$F_s, F_{c1}$ and $F_{c2}$	Attenuation Fix at 6 db

## 5. Result and Discussion

This section presents and discusses the magnitude response, phase response, minimum order and group delay for the studied IIR and FIR filters using the design parameters from Section 4.

### 5.1 IIR Magnitude Responses

Fig.1 shows the IIR magnitude response of the 2<sup>nd</sup> till 30<sup>th</sup> orders for the Butterworth, Chebyshev Type 1 and Elliptic filters. Here the magnitude is in dB, while the frequency is in Mega Hertz (MHz).

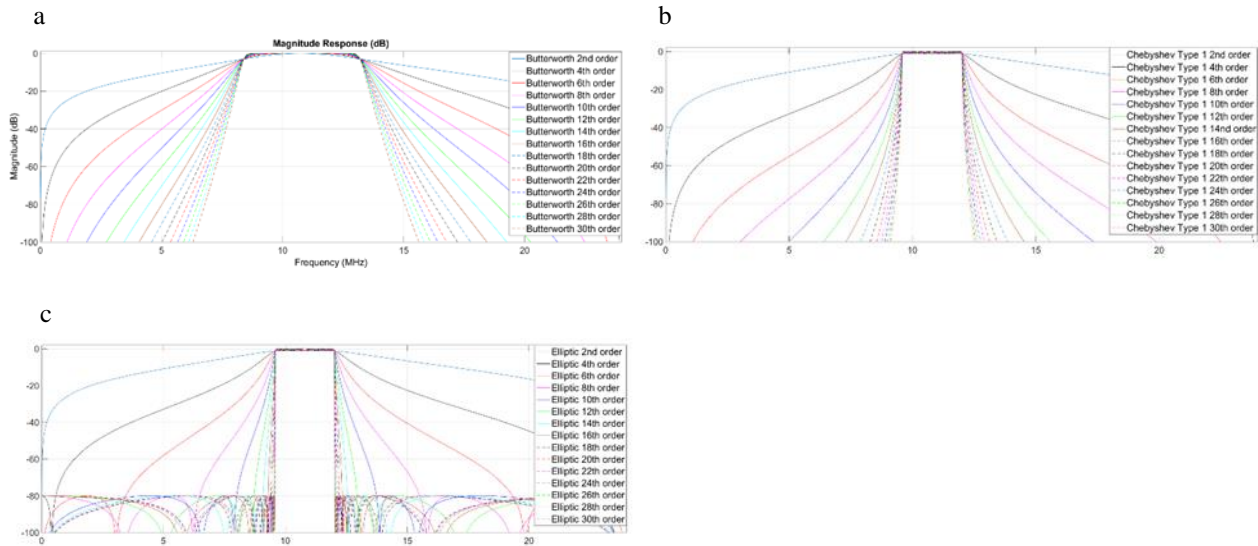


Fig. 1 - IIR magnitude response (a) Butterworth (b) Chebyshev Type 1 (c) Elliptic

The Butterworth magnitude responses have the slowest roll-off and the least steep magnitude response. However, the filter has no ripple in the passband and stopband. Due to this, the transition region of the filter is wider when compared to the others. The increase of the order filter demonstrates only slight changes to the roll-off of the magnitude response. Butterworth can be categorized as the simplest filter among the three studied filters. Based on Equations (2.1), (2.2) and (2.3), Butterworth is the only filter that has no ripples factor, selectivity factor and polynomial. The Chebyshev Type 1 filter performed moderately where the filter has only ripples at passband, while Elliptic filters have ripples at both passband and stopband

Among these three filters, Elliptic showed the steepest magnitude response, however, due to the ripple factor  $\epsilon$  and the selective factor  $\xi$ , the Elliptic filters have both ripples in the passband and stopband. In wireless communication, the filter must have a square response with no ripple in both stopband and passband to make it ideal. This is to preserve the waveforms of the signal from being filtered to the extent that it is impossible for the intended signals to be detected due to the filtering process. Therefore, preserving or recovering the originally transmitted waveform is of utmost importance or else wrong threshold decisions will be made, which results to a bit error in the communications system.

Table 3 shows the magnitude response for all three types of IIR filter. From the table, we can see the trade-off between the ripples and the roll-off of the filters. Note that if there are no ripples and low roll-off is low, the transition region is wide. The roll-off becomes steeper if there are ripples in both passband and stopband.

Table 3 – IIR Magnitude Response Analysis.

Attribute/Filter Types	Butterworth	Chebyshev	Elliptic
Ripples	Non	Large	Large
Roll-off	Lowest	Medium	Fastest
Group Delay	Yes	Yes	Yes
Transition Region	Large	Small	Small

### 5.2 FIR Magnitude Responses

Fig.2 shows the magnitude response for the studied FIR filters. The results demonstrate that all FIR filters required high filter orders to achieve the ideal response or to have a steep response. The roll-off for Bohman is the slowest as we increase the order but the ripple in the stopband is hard to see. The main weakness of Bohman filter is that the passband is huge, which can lead to the overlapping of adjacent symbols and cause the problem of ISI. Furthermore, if the passband is exceeding the designed parameters, the efficiency of bandwidth allocation is decreasing. For Hamming window filtering technique, the magnitude response can easily achieve near to ideal response with the increased of filter orders, the response of Hamming window even surpasses the roll-off of Bohman window. Having said that, as a trade-off, Hamming window generates ripples at stopband. The only filters that create ripples at stopband are Hamming window and Equiripple.

Finally, in terms of roll-off, Equiripple filters achieve the steepest magnitude response, but in return, it has high ripple in stopband. As the order increases, the ripple in stopband is getting cramped and the ideal response can be seen. At the particular point, we can see that in Fig. 2a, increasing the order yields only insignificant performance difference. Note that the Equiripple filter is the only FIR filter that has a sharp transition region by given parameters when compared to the other FIR filter tested.

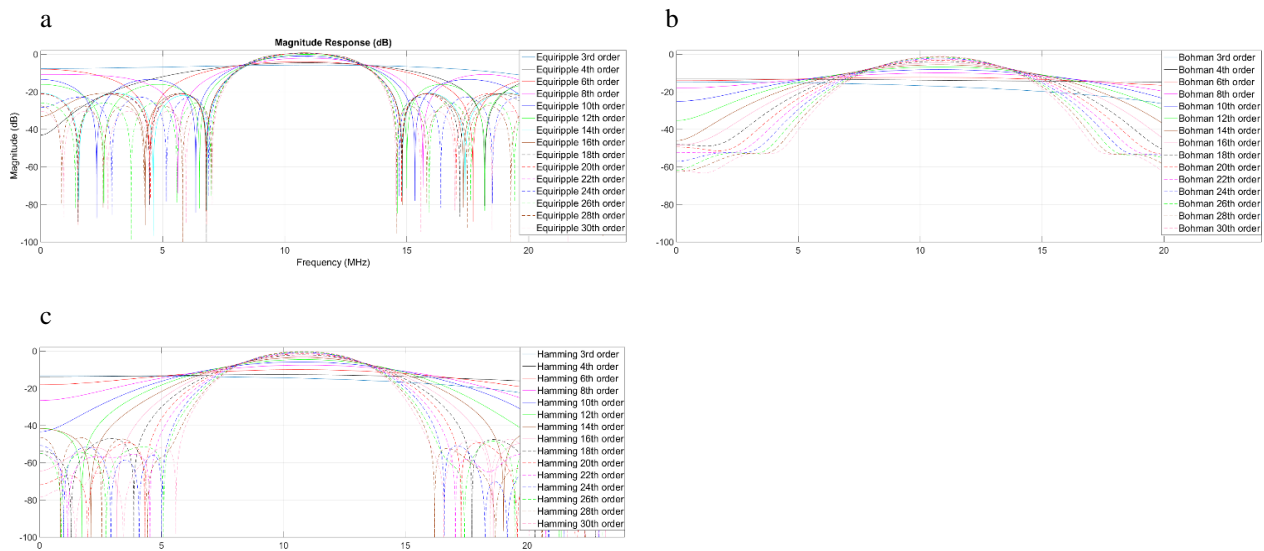


Fig. 2 - FIR magnitude responses for (a) Equiripple (b) Bohman (c) Hamming

Table 4 summarizes the roll-off in relation to the ripples on the stopband. We can see that steeper roll-off response contributes to the more ripples on the stopband. The transition region for all FIR filters can be considered as wide when compared to IIR filters. Among all studied FIR filters, Equiripple have the narrowest transition region. As we discuss in (5.1), square shape is important to preserve the original signal. Thus, transition region plays important role in shaping a square filter magnitude.

**Table 4 – FIR Magnitude Response Analysis.**

Attribute/Filter Types	Equiripple	Bohman	Hamming
Ripples at stopband	Large	Small	Medium
Transition region	Small	Largest	Large
Roll-off	Fastest	Lowest	Medium
Implementation cost(10 <sup>th</sup> filter order)	31	27	31

### 5.3 Phase Responses

Fig.3 shows the phase responses for the studied IIR and FIR filters. From the figure, it is clearly shown that all IIR filters do not have linear phase. As we run the simulation for the IIR filter, all phase is delayed (curve sloop) at every single point. Thus, it makes our point fulfilled that non-linear phase will cause group delay (refer to 5.3.1 and 5.3.2) as the phase are not linear. For FIR phase response, the phase is all linear, the group delays are constant (refer to 5.3.3 section), thus it makes FIR have no distortion but only a time delay staggantly

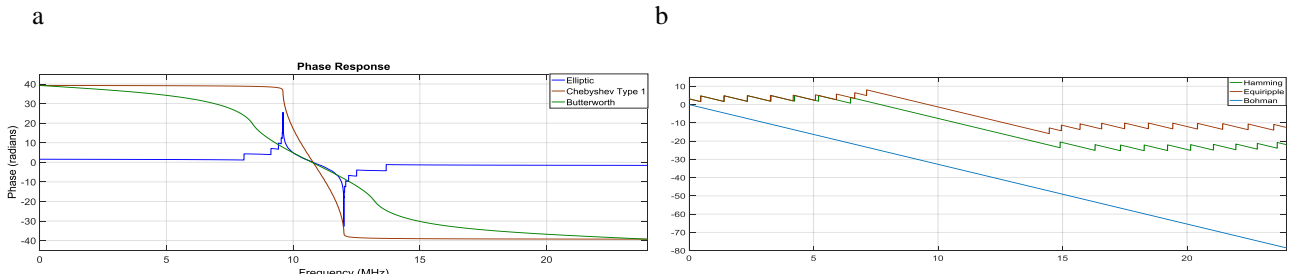


Fig. 3 – (a)IIR and (b)FIR 50<sup>th</sup> order phase response

Table 5 – FIR Magnitude Response Analysis.

Filter Types \ Frequency	9600kHz (rad)	10800kHz (rad)	12000kHz (rad)
Butterworth	$-7.6 \times 10^{-3}$	$5.5 \times 10^{-3}$	$7.0 \times 5.5 \times 10^{-3}$
Chebyshev Type 1	$-3.8 \times 10^{-3}$	$4.5 \times 10^{-3}$	$2.7 \times 10^{-3}$
Elliptic	$7.8 \times 10^{-4}$	$2.6 \times 10^{-4}$	$3.5 \times 10^{-4}$
Equiripple	3.3	3.3	3.3
Bohman	3.3	3.3	3.3
Hamming	3.3	3.3	3.3

Since the phase response for IIR is not linear, we choose 1st cut-off, 2nd cut-off and center sampling as our benchmark point. Table 5 shows that the phase responses of IIR are delay unevenly, which will cause frequency packets to experience difference delay at the output and this will lead information interpreted incorrectly at the output. Unlike the FIR filters, the phases are linear and the delay for each phase are even. We can conclude from this phase responses analysis, that the IIR are non-linear filters and the group delay for IIR filter are not even; while for FIR, the filters are a linear filter, so the group delay for FIR filter will be stagnant. The non-linear phase IIR filter changes the frequency component of the signal such that different shape of signals is obtained at the output when compared back with the input.

### 5.4 IIR and FIR Group Delay Analysis

The results present for all three IIR 20<sup>th</sup> filter order and minimum filter order group delay, for FIR filter we only simulate for 50<sup>th</sup> filter order. This is because after we simulate the phase response (5.3), we conclude that all FIR filter has a linear phase response. The linear phase response leads to stagnant group delay. In contrast, all of the IIR filters have delay whereby Butterworth filter demonstrates the highest delay followed by Chebyshev and Elliptic.

#### 5.4.1 IIR 20<sup>th</sup> Filter Order Group Delay

Table 6 summarizes the group delay in 20<sup>th</sup> filter order for all IIR filter. We choose 20<sup>th</sup> order because we select one fix filter order and we also select one minimum order for all 3 filters (5.4). We selected the highest samples that delay during the simulation. We notice that all the samples that delay are at the cut-off frequency ( $F_c$ ) and at frequency stop ( $F_{stop}$ ). This is due to the poles that rise in  $F_c$  and  $F_{stop}$ , we can conclude that the highest samples delay occur when poles are rising. The Elliptic filter reveals the highest sample that delayed. There are 860 samples delayed only at 9.6 MHz and followed by Chebyshev 338 samples at 9.6 MHz and Butterworth has 44 samples delayed at 8.4 MHz. However, for the minimum order, Chebyshev achieves the highest samples delayed followed by Butterworth and Elliptic.

Table 6 – 20<sup>th</sup> Filter Order Group Delay.

Filter	Highest delay for 1 <sup>st</sup> cut off	Highest delay for 2 <sup>nd</sup> Cut off
Butterworth	44 samples @ 8.4Mhz	40 samples @ 13 Mhz
Chebyshev Type 1	338 samples @ 9.6Mhz	324 samples @ 11 Mhz
Elliptic	860 samples @ 9.6Mhz	812 samples @ 12 Mhz

### 5.4.2 IIR Minimum Order Group Delay

Table 7 presents the minimum order for the chosen IIR filters. In general, the Elliptic filter outperforms the Butterworth and Chebyshev filters. The Elliptic filter only requires 10<sup>th</sup> order to achieve the magnitude response nearly to an ideal filter while Butterworth and Chebyshev require 18<sup>th</sup> and 12<sup>th</sup> filter order, respectively. Furthermore, Elliptic demonstrates the lowest delay at 1<sup>st</sup> cut off, 55 samples, compared with Butterworth, 64 samples, and Chebyshev, 110 samples.

**Table 7 – Nearly Ideal Filter Group Delay.**

Filter	Highest delay for 1 <sup>st</sup> Cut off	Highest delay for 2 <sup>nd</sup> cut off
Butterworth (18 <sup>th</sup> filter order)	64 samples @ 9.5Mhz	61 samples @ 12 Mhz
Chebyshev Type 1 (12 <sup>th</sup> filter order)	110 samples @ 9.6 Mhz	105 samples @ 11.9 Mhz
Elliptic (10 <sup>th</sup> filter order)	55 samples @ 9.5 Mhz	53 samples @ 12 Mhz

### 5.4.3 FIR 50<sup>th</sup> Order Group Delay

Table 8 shows the group delay for FIR are consistent due to the linear phase of FIR property regardless of any filter order the delay are stagnant as stated in (5.3). All the FIR filters tested revealed that the delay increases as the filter order increases, but the delay stays stagnant over the frequency, as shown in Fig.4 and Table 5

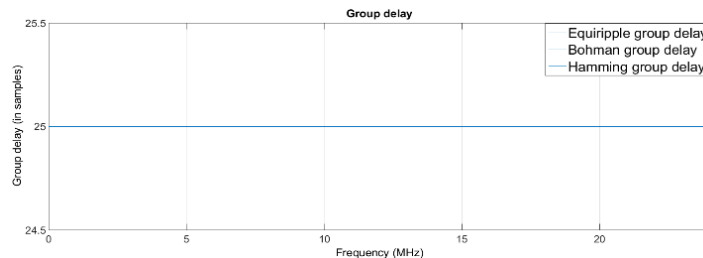


Fig. 4 - 50<sup>th</sup> order group delay for all tested FIR

**Table 8 – Nearly Ideal Filter Group Delay.**

Filter(order 50 <sup>th</sup> )	Highest delay for 1 <sup>st</sup> cut off	Highest delay for 2 <sup>nd</sup> Cut off
Equiripple	25 samples	25 samples
Bohman	25 samples	25 samples
Hamming	25 samples	25 samples

### 5.4.4 Minimum Filter Order for Nearly Ideal Magnitude Response

Fig.5 shows the magnitude responses for the minimum filter order of IIR and FIR, which are characterized nearly as an ideal filter. In general, the IIR achieves the steepest transition region and has narrow bandpass compared to FIR. The IIR filters, namely, Butterworth, Chebyshev, and Elliptic required 18<sup>th</sup>, 16<sup>th</sup> and 10<sup>th</sup> order respectively to filter 4.8 MHz sample, as shown in Fig.5(a). In spite of high 50<sup>th</sup> filter order for all FIR, high ripple and wide main lobe can still be seen in Fig.5(b). The transition region that exceeds 4.8 MHz or any specification for bandpass will cost ISI issue. Because of previous side lobes and ripples that filter let it pass thru, it will create more ISI for next frequency sampling. This process will keep on going until the sampling process done at both transmit and receive that will cost high SNR and high delay.

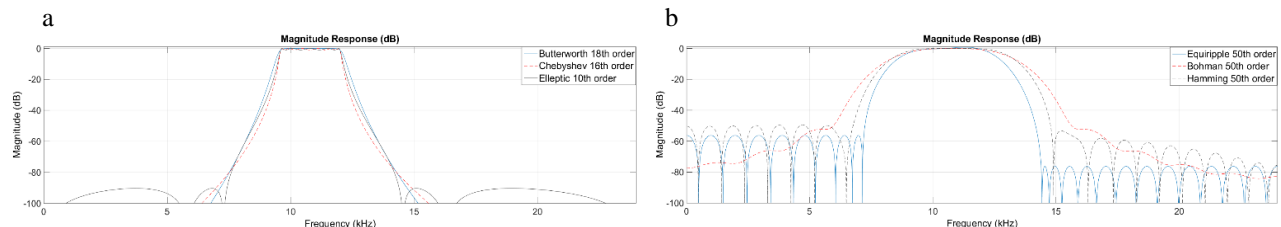


Fig. 5 - Nearly ideal filter with individual filter order (a) Butterworth 18<sup>th</sup> order, Chebyshev 16<sup>th</sup> order and Elliptic 10<sup>th</sup> order. (b) Equiripple, Bohman and Hamming 50<sup>th</sup> order

The filter characterised with narrow transition region will make the magnitude response of the obtained filters fade out quickly and thus the ISI problem is likely to occur between consecutive OFDM symbols. When ISI presents we required long CP to mitigate the delay to make sure that good system performance can be achieved. Due to the fastest roll-off and small transition region at low order (i.e. 10), Elliptic seems to be a feasible filter to be applied in the f-OFDM, particularly in the 5G communication.

## 6. Conclusion

This paper presented a comparative study between IIR and FIR in terms of magnitude response, phase response, group delay, and the minimum filtering order to achieve near ideal filter responses. The results showed that the IIR filter has the steepest transition region when compared to the FIR filter designed using the same order. The reason behind this result is driven by the relationship between the values of the IIR filter order and the number of poles in the unit circle. We concluded that IIR filters with more poles in a unit circle have steeper roll-off. Among all the studied IIR filters in this work, we found that Elliptic is the most suitable candidate for the filtered-OFDM systems. This is because the Elliptic is able to suppress the side lobe and to minimize the ripples in stopband with only a minimum order of 10th. The order of the filter is important to be considered so that the implementation can doable in the real 5G system.

While IIR filters are superior in the magnitude response, the FIR filters have better and linear delay response. Here it is important to have a linear phase in the filter so that the output of the signal experienced less distortion. For FIR filter, Equiripple filters show the outstanding result when compared to Bohman and Hamming where they have fastest roll-off and narrowest transition region with similarly designed parameters.

## Acknowledgement

The research work is supported by the Ministry of Education Malaysia, High Center of Excellence Wireless Communication Center (WCC) and Ubiquitous Broadband Access Networks (U-BAN) research group in Universiti Teknologi Malaysia under grants R.K130000.7840.4J235 and Q.K130000.2540.18H25.

## References

- [1] H. K. Kwan, "Variable Multi-output Passive Digital Filters," 2005 IEEE International Symposium on Circuits and Systems, Kobe, 2005, pp. 3725-3728 Vol. 4.
- [2] A. Gupta and R. K. Jha, "A Survey of 5G Network: Architecture and Emerging Technologies," in *IEEE Access*, vol. 3, pp. 1206-1232, 2015.
- [3] P. Marsch *et al.*, "5G Radio Access Network Architecture: Design Guidelines and Key Considerations," in *IEEE Communications Magazine*, vol. 54, no. 11, pp. 24-32, November 2016.
- [4] E. Hossain and M. Hasan, "5G Cellular: Key Enabling Technologies and Research Challenges," *IEEE Instrum. Meas. Mag.*, vol. 18, no. 3, pp. 11\_21, Jun. 2015.
- [5] S. Han, Y. Sung and Y. H. Lee, "Filter Design for Generalized Frequency-Division Multiplexing," in *IEEE Transactions on Signal Processing*, vol. 65, no. 7, pp. 1644-1659, 1 April, 2017.
- [6] Z. He, L. Zhou, Y. Chen and X. Ling, "Filter Optimization of Out-of-Band Emission and BER Analysis for FBMC-OQAM system in 5G," *2017 IEEE 9th International Conference on Communication Software and Networks (ICCSN)*, Guangzhou, 2017, pp. 56-60.
- [7] K. Surma-Aho and T. Saramaki, "A Systematic Technique for Designing Approximately Linear Phase Recursive Digital filters," in *IEEE Transactions on Circuits and Systems II: Analog and Digital Signal Processing*, vol. 46, no. 7, pp. 956-963, July 1999.
- [8] Laka Barik and Asutosh Kar. "ICI Self-Cancellation Method of BPSK OFDM," *IJCA Proceedings on International Conference on VLSI Communications and Instrumentation (ICVCI)* (15):12-14, 2011.
- [9] A. Steegen, "Technology innovation in an IoT era," 2015 Symposium on VLSI Technology (VLSI Technology), Kyoto, 2015, pp. C170-C171

- [10] A. Ijaz *et al.*, "Enabling Massive IoT in 5G and Beyond Systems: PHY Radio Frame Design Considerations," *IEEE Access*, vol. 4, pp. 3322– 3339, 2016.
- [11] J. G. Proakis, D. G. Manolakis: *Digital Signal Processing: Principles, Algorithms, and Applications*, Prentice Hall, 2007, 4th edition
- [12] S. K. Mitra: *Digital Signal Processing: A Computer Based Approach*, McGraw Hill Higher Education, 2006, 3rd edition.
- [13] A. U. Haque, "Comparing Chebyshev and Butterworth Filter for Designing 2-D Recursive Digital Filter," 2005 Pakistan Section Multitopic Conference, Karachi, 2005, pp. 1-5.
- [14] N. B. Rizvandi, M. R. N. Ranjbar and M. M. nejad, "Approximation of IIR Filters with Equivalent FIR Filters in Magnitude and Group Delay Responses," 2007 15th International Conference on Digital Signal Processing, Cardiff, 2007, pp. 288-291.
- [15] N. Sokhandan and S. Mostafa Safavi, "Sidelobe Suppression in OFDM-Based Cognitive Radio Systems," *Information Sciences Signal Processing and Their Applications (ISSPA)*, 2010 10th International Conference on Kuala Lumpur, 2010, pp. 413-417.
- [16] W. S. Lu and A. Antoniou, "Design of Digital Filters and Filter Banks by Optimization: A State of The Art Review," 2000 10th European Signal Processing Conference, Tampere, Finland, 2000, pp. 1-4.
- [17] R. Pal, "Comparison of The Design of FIR and IIR Filters for a Given Specification and Removal of Phase Distortion from IIR filters," 2017 International Conference on Advances in Computing, Communication and Control (ICAC3), Mumbai, India, 2017, pp. 1-3.
- [18] K. Yamamoto and K. Suyama, "Active Enumeration of Local Minima for IIR Filter design using PSO," 2017 Asia-Pacific Signal and Information Processing Association Annual Summit and Conference (APSIPAASC), Kuala Lumpur, 2017, pp. 910-917.
- [19] S. Ohno, M. R. Tariq and M. Nagahara, "Min-Max IIR Filter Design for Feedback Quantizers," 2017 Asia-Pacific Signal and Information Processing Association Annual Summit and Conference (APSIPAASC), Kuala Lumpur, 2017, pp. 938-942.
- [20] F. Serbet, T. Kaya and M. T. Ozdemir, "Design of Digital IIR Filter using Particle Swarm Optimization," 2017 40th International Convention on Information and Communication Technology, Electronics and Microelectronics (MIPRO), Opatija, 2017, pp. 202-204.
- [21] S. A. Jadhav, S. B. Misal, A. Mishra and A. Murugkar, "Designing of Stepped Impedance Butterworth and Chebyshev Filters for Wireless Communication," 2017 IEEE Applied Electromagnetics Conference (AEMC), Aurangabad, 2017, pp. 1-2.
- [22] A. S. Ali, A. G. Radwan and A. M. Soliman, "Fractional Order Butterworth Filter: Active and Passive Realizations," in *IEEE Journal on Emerging and Selected Topics in Circuits and Systems*, vol. 3, no. 3, pp. 346-354, Sept. 2013.
- [23] R. A. Wood and N. B. Jones, "Generalised Chebyshev Lowpass Filters," in *Electronics Letters*, vol. 4, no. 8, pp. 158-159, April 19 1968.
- [24] S. A. Rathod and S. Yellampalli, "Design of Fifth Order Elliptic Filter with Single-Opamp Resonator," 2014 International Conference on Advances in Electronics Computers and Communications, Bangalore, 2014, pp. 1-6.
- [25] I. W. Selesnick, M. Lang and C. S. Burrus, "Magnitude squared design of Recursive Filters with The Chebyshev Norm Using a Constrained Rational Remez algorithm," *Proceedings of IEEE 6th Digital Signal Processing Workshop*, Yosemite National Park, CA, 1994, pp. 23-26.
- [26] M. Mukherjee, L. Shu, V. Kumar, P. Kumar and R. Matam, "Reduced Out- of-Band Radiation-Based Filter Optimization for UPMC systems in 5G," 2015 International Wireless Communications and Mobile Computing Conference (IWCMC), Dubrovnik, 2015, pp. 1150-1155.
- [27] A. Basit, I. M. Qureshi, W. Khan, S. u. Rehman and M. M. Khan, "Beam Pattern Synthesis for an FDA Radar with Hamming Window-Based Nonuniform Frequency Offset," in *IEEE Antennas and Wireless Propagation Letters*, vol. 16, pp. 2283-2286, 2017.